UCRL-JC-131240
PREPRINT

Modeling Line Emission from ICF Capsules in 3 Dimensions

S. H. Langer, H. A. Scott, M. M. Marinak, O. L. Landen

This paper was prepared for submittal to
Journal of Quantitative Spectroscopy and Radiative Transfer

February 11, 1999

Lawrence Livermore National Laboratory

Modeling Line Emission from ICF Capsules in 3 Dimensions

Steven H. Langer, Howard A. Scott, Michael M. Marinak, and Otto L. Landen

Lawrence Livermore National Laboratory, University of California, Livermore, CA 94550

Abstract--Hydrodynamic instabilities can reduce the yield in inertial confinement fusion (ICF) implosions. Line emission from dopants placed in the capsule can be used to diagnose the extent of the instabilities. In an earlier paper[1] we compared line emission measured in experiments performed on the Nova laser to 1D mix models and 2D models in which many different instability wavelengths interact. Three-dimensional simulations are required to model properly the saturation of the hydrodynamic instabilities. This paper presents the results of the first 3D simulations of line emission from ICF capsules. The simulations show that the three lines considered here come from different spatial regions. Line ratios cannot be used to determine temperatures without accounting for the spatial dependence of the line emission. Future papers will present detailed comparisons to experiments.

1. INTRODUCTION

Mix due to hydrodynamic instabilities is important in inertial confinement fusion (ICF) implosions because it can reduce the thermonuclear yield. One of the techniques that has been developed for studying these instabilities is to measure the line emission of dopants placed in the fusion capsule. In the experiments discussed here, argon was placed in the DH fuel in the center of the capsule and titanium was placed in the inner layers of the plastic shell. Argon line emission is strong at the time of peak compression when the DH is both hot and dense, and serves as an indicator of the temperature in the fuel. Titanium emission is weak if the implosion is symmetric (the plastic all remains cool). If the interface between the fuel and the plastic shell becomes highly distorted, titanium emission will increase as the parts of the shell that poke furthest inward are heated due to their close proximity to the hottest parts of the fuel. The emission from titanium is thus a signature of a distorted shell.

One issue that has arisen in the past is whether hydrodynamic instabilities grow large enough to lead to the development of a turbulent layer in which shell and fuel material atomically mix, or whether the instabilities lead to a distorted interface between the fuel and the shell. Previous simulations have shown that most of the reduction in thermonuclear yield is due to distortions with wavelengths that are roughly one-twentieth of the shell circumference. These wavelengths are modeled in the hydrodynamic simulations used in this paper.

The growth rate of hydrodynamic instabilities increases as the wavelength decreases, and may lead to the development of turbulence at short wavelengths if stabilizing processes such as heat conduction are not important. This turbulent layer (if it exists) is very thin compared to the fuel radius, so it has little effect on thermonuclear yield. Turbulence probably will have little effect on the strength of argon lines, but it might be significant for titanium line emission. We hope to address this question in future papers.

In an earlier paper[1] we compared line emission measured in experiments performed on the Nova laser to 1D mix models and 2D models in which many different instability wavelengths interacted. The 2D models came closer to matching the experimental data than the 1D mix models, but the predictions for line emission from titanium in the plastic shell were not in close agreement with the data. The models showed that the line emission was dominated by the portions of the plastic shell that poked furthest into the hot fuel. Rayleigh-Taylor instabilities saturate differently in three dimensions than in two dimensions (Marinak[2] et al. 1995 and references 7-14 therein). This suggests that there could be significant differences in predicted line emission from the shell between 2- and 3-dimensional models. This paper presents the results of the first 3-dimensional simulations of line emission from ICF capsules. These simulations are extremely demanding computationally, so we include a discussion of some of the issues involved in the modeling. We also present basic results from our simulations. Future papers will present detailed comparisons to experiments.

2. THE MODELING PROCEDURE

ICF capsules have imperfections on both their inner and outer surfaces. Perturbations on the outer surface grow due to the Rayleigh-Taylor instability[3,4] during the inward acceleration of the capsule and feed through to perturb the inner surface. Perturbations at the inner surface grow due to the Rayleigh-Taylor instability when the shell decelerates near the time of peak compression. Richtmeyer-Meshkov instabilities[5,6] occur as shocks pass through the capsule and cause the growth of perturbations on the inner surface which seed Rayleigh-Taylor instabilities when the shell decelerates.

The initial surface perturbations can be broken down into normal modes. Different modes grow at different rates and will interact with one another if their amplitudes grow out of the linear regime (i.e. the amplitude becomes comparable to the wavelength). The number of zones in the computational grid is controlled by the instability wavelengths that must be resolved.

Two different capsules are modeled in this paper. The first is a Nova capsule, which has large (3D) angular variations in the x-ray drive radiation and a smooth capsule. The second is an Omega capsule with perturbations on the capsule surface and more modest asymmetries in the x-ray drive radiation. Figure 1 shows the Nova and Omega capsules. The capsules are driven by x-rays generated in a standard Nova hohlraum (see Lindl[7] for a discussion of the Nova laser facility). The hohlraum for the Nova simulation is driven by a 2.0 ns laser pulse with 32 kJ of 0.35 μm light. There is an intensity contrast of 5 between the low intensity foot of the pulse and the main drive pulse. The capsule has germanium in the outer portion of the plastic shell to absorb hard x-rays and prevent pre-heat of the plastic. Argon is placed in the DH fuel and titanium is placed in the innermost part of the plastic shell. The argon and titanium concentrations are low enough that they do not change the implosion hydrodynamics, but their line emission serves as an indicator of conditions in the capsule.

The radiation drive asymmetry for the Nova capsule is based on experimentally measured beam-to-beam power imbalances and pointing errors as well as the intrinsic time-dependent P2 and P4 drive asymmetries in the hohlraum[8]. To provide the asymmetric x-ray drive for a particular simulation, a set of random numbers is used to choose specific beam pointing errors from the experimental distribution. This is combined with P2 and P4 asymmetries from a 2D Lasnex[9] hohlraum simulation to generate an angle- and time-dependent x-ray source. In the particular simulation performed for this paper, the drive asymmetry was quite large (but not outside the range that is expected for Nova). The effect of the surface perturbations present on the capsule would have been much smaller than that of the drive asymmetry, so we used a perfectly smooth capsule in the simulation. Most of the results presented in this paper are for the Nova capsule because the large distortions lead to interesting features in the line emission.

The Omega capsule is similar to the Nova capsule. The laser energy is reduced to 15 kJ, the laser pulse length is 2.4 ns, and the shell thickness was reduced to 30 μm. The capsule has an RMS surface perturbation of 0.2 μm on its outer surface, corresponding to the best capsules currently available. The x-ray drive asymmetry is based on estimates of the Omega laser, and is much smaller than that in the Nova simulation.

Line emission is modeled using a 3D radiation-hydrodynamics code called HYDRA [10] and an atomic kinetics code called Cretin[11]. HYDRA solves the radiation-hydrodynamics equations to model the implosion of the ICF capsule. Temperature and density profiles from HYDRA are passed to Cretin, which solves the atomic kinetics equations for the populations of the atomic configurations simultaneously with the radiation transport equations for the Helium- and Lyman-α lines. All other lines are assumed to be optically thin.

The HYDRA models were run on 8 processors of a Cray J-90 vector supercomputer, and require roughly 10 days to complete (highly perturbed capsules take longer). The Cretin models were run on a 625 MHz DEC 8400 multiprocessor RISC compute server. The Cretin simulations take roughly 10 CPU hours per time step (10 time steps around peak compression capture all significant line emission).

The HYDRA models include Legendre modes 2-20 (in the case of the Omega capsule), which are the only modes expected to contribute significantly to the perturbations of the fuel/pusher interface. The Nova model uses 166 radial zones, 32 zones in polar angle, and 64 azimuthal zones and covers two octants. The Omega simulation covers only one octant, so P_1 perturbations are modeled as P_2 perturbations. The Omega model uses 166 radial zones, 96 zones in polar angle, and 64 azimuthal zones. The HYDRA models use three carefully chosen photon frequencies with weighted opacities that are calculated from a 1D implosion run with a large number of frequency groups[12]. The use of these weighted opacities avoids the prohibitively large run times that would result from using many frequency groups in the 3D simulation. The HYDRA simulation uses an orthogonal grid with a region of finely spaced radial zoning that follows the motion of the shell. HYDRA uses an interface tracker to minimize diffusion at the material boundary between the fuel and the shell.

Cretin uses an atomic database from the Ration code[13] for both argon and titanium. This database has 70 configurations for hydrogen-like, helium-like and doubly excited lithium-like configurations, as well as hydrogenic ground-state configurations for less ionized stages. The compressed fuel reaches electron densities exceeding 10^{24} cm^{-3}, so both Stark broadening and continuum lowering are important[14]. Stark broadening is handled by including an appropriate width in the calculation of the Voigt profile for each line. The width is obtained from fits to detailed line shape calculations[15] where applicable, and from theoretical formulas[16] for the remaining lines. Continuum lowering is handled in a Stewart-Pyatt approximation[14] that has been modified so configurations disappear smoothly as the density is varied. The spectra use 282 frequencies so that the individual lines can be resolved.

The argon He-α, argon Ly-α and perhaps the titanium He-α lines are optically thick in these capsules, while all other lines are optically thin. Earlier work[17,18] has shown that the strength of the argon β lines is affected by optical depth effects in the α lines. These effects are self-consistently included in the line transfer calculation of the He-α and Ly-α lines[11]. We have included the continuum opacity of the shell material in some of these simulations.

The numerical grid has been reduced to 120 radial zones, 32 zones in polar angle, and 32 azimuthal zones when the temperature and density from HYDRA are fed into Cretin. This was necessary to make the simulation fit into the memory of the computers available to us (see section 3). The effects of this approximation should not be large because the reduced grid still resolves the perturbation wavelengths with the largest amplitudes, and couplings with shorter wavelengths were included in the HYDRA simulations.

3. COMPUTATIONAL ISSUES

Cretin has been able to model the radiation transport of lines in two dimensions for several years. The 2D line transfer package tracks lines in three dimensions through the two dimensional grid, so the extension to a 3D grid was reasonably straightforward. The greatest difficulty associated with moving to three dimensions is the large increase in memory needed to run a simulation. The 32x32x120 zone problem (with carbon) described in this paper requires 4.3 GB of memory when run on 2 processors of a DEC 8400.

Cretin can be run in parallel using either shared memory techniques or by passing messages on a distributed memory computer using MPI. Cretin achieves good parallel speed-up for the non-LTE atomic kinetics with either form of parallelism and the memory demands do not change rapidly with the number of processors.

The 2D/3D line transfer package in Cretin currently is parallel over lines when using distributed memory and over directions when using shared memory. Each processor participating in a distributed memory parallel run needs roughly 1.8 GB (for the problem mentioned above) to carry out the radiative transfer of a line. We have not yet run these simulations on a distributed memory computer because we do not have access to one with sufficient memory on each node. The memory requirements for a parallel run on a shared memory computer are much more reasonable – each additional processor increases the memory requirements by a few hundred MB. All of the results presented in this paper were obtained using 2 CPUs of a DEC 8400. The 8400 has 8 processors, but the load on the computer prevented us from using more than 2 in these runs. The argon and titanium emission is computed in separate Cretin runs.

One method for dealing with the large per-processor memory requirements is to replace the current radiation transfer package in Cretin with a package that spatially decomposes the grid. The memory requirement per CPU will drop as the grid is split into more pieces, so the memory per CPU will not be a problem if many CPUs are employed. Spatially decomposed radiation transport requires iterative methods to handle correctly the coupling between the different spatial domains, so it is not as efficient as the scheme currently used in Cretin. We anticipate that in the future we will use spatially decomposed radiation transport for large problems and the current scheme for smaller jobs.

4. RESULTS

A first step in understanding the emission line strengths is to determine where they are emitted. Figure 2 shows the density of the upper state populations from the Omega simulation for the argon Ly-α and He-α lines. The argon in the center is mostly hydrogenic, while helium-like argon occurs only in the cooler portions of the fuel close to the shell. This distribution of ionization stages means that the argon Ly-α line is emitted throughout the hot fuel, while the He-α line is emitted from a thin layer adjacent to the shell. Figure 3 shows the equivalent image for the Nova capsule. In this capsule, the emission of the argon Ly-α line is weak at the center because the fuel is hot enough that most of the argon in the center is fully stripped. The distribution of argon line emission is otherwise similar to that for the Omega capsule. The titanium He-α line for both capsules is emitted from an extremely thin layer at the inner surface of the shell, and the strongest emission comes from the points where the shell comes closest to the center of the capsule.

These results show that it will be difficult to use ratios between the two argon lines as a temperature diagnostic (because they are emitted in different places) without using detailed hydrodynamic modeling. The spatial separation is smaller at times before and after peak fuel temperature when the fuel is not hot enough to fully ionize argon.

X-ray images of the capsule are one technique that can be helpful in understanding an implosion. Figure 4 shows images of the argon He-α line and figure 5 shows images of the argon Ly-α line from the Nova capsule in four different directions. The images are normalized to the peak brightness of each line. The He-α images vary enough between directions that experiments might be able to detect the effect (for a capsule, like this one, that has large drive asymmetry). The Ly-α images are smoother than those for the He-α line, but are still not round.

Figure 6 shows images of the Nova capsule in the titanium He-α line from four different directions. The brightest spot in the image from the y-direction is significantly brighter than any spot in the other three images. The peak brightness is greater in some directions than in others because the emission comes from extremely thin small spots that appear dimmer when viewed side-on.

Figure 7 shows the He-α line from the Nova simulation seen along the y-axis with and without the effects of emission and absorption of carbon in the plastic shell. Earlier estimates indicated that absorption in the plastic shell might significantly alter line strengths and even line ratios. The differences are relatively minor in this case, but might become significant if less shell material were ablated away. The germanium in some ICF capsules is limited to the outer portions of the shell and all ablates away during the implosion. If germanium is present throughout the shell, its opacity may be high enough to affect line strengths.

Figure 8 shows line-outs along the y-axis of the upper state populations for all three lines. The argon Ly-α line has a broad peak and drops by only a factor of 2 at the center. The argon He-α line has a narrow peak near the outer edge of the fuel. The titanium He-α line has a 1 zone wide peak that is barely visible at y=25 μm. The resolution in the region where the titanium is emitted needs to be increased and this could be done by adding more radial zones. Another approach is to use the new ALE (arbitrary Lagrange-Eulerian) hydrodynamics option in HYDRA to have the grid lines follow the distorted interface between the fuel and the shell (in contrast to the orthogonal grids used in these simulations). Fine spatial resolution would then only be needed in a thin band next to the interface, not over the entire radial region spanned by the interface.

The titanium line strength is very sensitive to direction. Figure 9 shows line-outs in several directions for the upper-state density of the titanium He-α line. The maximum density among these directions is only 7% of the maximum over all directions, whereas the argon lines reached 60% of their maximum in the single direction shown in figure 8. This is consistent with the patchy nature of the titanium image in figure 6.

There are several differences in the spectrum between the Nova and Omega capsules that are related to the lower ionization state of the Omega capsule. Figure 10 shows the spectrum at the time of peak emission for all three capsules (viewed along the +x-axis). The 50 atmosphere Omega capsule has He-α lines that are the same strength as those of the Nova capsule, while its He-α satellite emission is stronger. This indicates that there was additional cool material in the Omega capsule.

Figure 11 shows the spectrum from the Nova simulation in 4 different directions. There are large angular variations in the line emission. The emission from the Omega capsules is essentially the same in all directions, so it is not shown.

5. SUMMARY

This paper has presented calculations of line emission from argon placed in the DH fuel and titanium placed in the inner layers of the plastic shell of an ICF capsule. The temperature and density are modeled using HYDRA and the line emission is calculated using Cretin. The most important result of this paper is the demonstration that it is possible to model line emission from 3D simulations that include the growth and interaction of many different perturbation wavelengths and the effects of asymmetry in the x-ray drive radiation. We have shown that the hydrogen- and helium-like lines of argon come from different spatial regions, making it difficult to use the ratio of argon He-β to argon Ly-β as a temperature diagnostic without the use of detailed hydrodynamic models. The titanium line emission comes from an extremely thin layer adjacent to the hot fuel and comes primarily from points where "fingers" of plastic poke into the fuel. Accurate modeling of the titanium emission will require increased spatial resolution at the boundary between the fuel and the plastic shell and perhaps the inclusion of a thin "turbulent" layer due to short wavelength Rayleigh-Taylor instabilities. In future papers, we will make a detailed comparison between 3D simulations and experimental data.

Acknowledgments --This work was performed under the auspices of the U. S. Department of Energy by the Lawrence Livermore National Laboratory under Contract No. W-7405-ENG-48.

REFERENCES

1. S. H. Langer, H. A. Scott, C. J. Keane, O. L. Landen, and Michael M. Marinak, *JQSRT* **58**, 709 (1997).

2. M. M. Marinak, B. A. Remington, S.V. Weber, R. E. Tipton, S. W. Haan, K. S. Budil, O. L. Landen, J. D. Kilkenny, and R. Wallace, Phys. Rev. Lett. **75**, 3677 (1995).

3. Lord Rayleigh, *Scientific Papers*, Vol. II, p. 200. Cambridge University Press (1990).

4. G. I. Taylor, *Proc. R. Soc. Lond. Ser. A* **201**, 192 (1950).

5. R. D. Richtmyer, *Commun. Pure Appl. Math.* **13**, 297 (1960)

6. E. E. Meshkov, *Izv. Akad. Nauk. SSSR. Mekh. Zhidk. Gaz.* **5**, 151 (1969) (NASA TTF-13-074, 1970).

7. J. D. Lindl, *Phys. Plasmas* **2**, 11 (1995).

8. "3-D Hydrodynamic Effects of Pointing and Power Balance Errors on Nova Capsule Implosions", M. M. Marinak, and S. P. Hatchett, *Bulletin of the APS* **41**, 1554 (1996) and UCRL-JC-124672 (contact the authors for copies).

9. G. B. Zimmerman, and W. L. Kruer, *Comm. Plasma Phys. Cont. Thermonuclear Fusion.* **2**, 51 (1975).

10. M. M. Marinak, R. E. Tipton, O. L. Landen, T. J. Murphy, P. Amendt, S. W. Haan, S. P. Hatchett, C. J. Keane, R. McEachern, and R. Wallace, *Phys. Plasmas* **3**, 2070 (1996).

11. H. A. Scott and R. W. Mayle, *Applied Physics B* **58**, 36 (1994). (Please note that Cretin and GLF use the same atomic kinetics package).

12. M. M. Marinak, R. E. Tipton, B. A. Remington, S. W. Haan, and S. V. Weber, National Technical Information Service Document DE-96004569, (1995 ICF Quarterly Report, UCRL-LR-105821-95-3). Copies can be ordered from the National Technical Information Service, Springfield, VA 22161.

13. R. W. Lee, B. L. Whitten, and J.E. Strout III., *JQSRT* **32**, 91 (1984).

14. C. J. Keane, G. W. Pollak, R. C. Cook, T. R. Dittrich, B. A. Hammel, O. L. Landen, S. H. Langer, W. K. Levedahl, D. H. Munro, H. A. Scott, and G. B. Zimmerman, *JQSRT* **54**, 207 (1995).

15. R. W. Lee, *J. Appl. Phys.* **58**, 612 (1985).

16. H. Griem, private communication.

17. C. J. Keane, B. A. Hammel, A. L. Osterheld, R. W. Lee, D. R. Kania, L. J. Suter, R. C. Mancini, C. F. Hooper Jr., and N. D. Delamater, *JQSRT* **51**, 147 (1994).

18. C. J. Keane, B. A. Hammel, D. R. Kania, J. D. Kilkenny, R. W. Lee, A. L. Osterheld, L. J. Suter, R. C. Mancini, C. F. Hooper Jr., and N. D. Delamater, *Phys. Fluids B* **5**, 3328 (1993).

Figure Captions

Figure 1. The capsules modeled in this paper have plastic shells filled with DH gas (fuel). The inner portion of the plastic shell is doped with titanium and the fuel is doped with argon. The plastic shell has a small amount of germanium to prevent higher energy drive x-rays from penetrating deep into the shell. The Nova capsule (left) has a thickness of 45 μm and the Omega capsule (right) has a thickness of 30 μm. The surface of the Nova capsule is perfectly smooth while the surface of the Omega capsule has an RMS roughness of 0.2 μm.

Figure 2. The density in the Omega capsule of the upper state for the argon Ly-α and He-α lines is shown in false-color. The upper half of the figure shows the density in the xz-plane and the lower half shows the density in the xy-plane. The Omega simulation covers an octant.

Figure 3. Same as figure 2, but for the Nova capsule. The fuel is hot enough at the center that the argon is completely ionized. The Nova simulation two octants.

Figure 4. Images of the Nova capsule in the argon He-α line from four different directions. The images are normalized to the peak brightness of the line. The images are not round and are significantly dimmer when viewed from the positive x direction.

Figure 5. Images of the Nova capsule in the argon Ly-α line from four different directions. The images are normalized to the peak brightness of the line. The images are smoother than for the He-α line, but are still not round.

Figure 6. Images of the Nova capsule in the titanium He-α line are shown from four different directions. The images are normalized to the peak brightness of the line. The images have many small "hot spots" (see especially the image from the y-direction) and vary greatly from one direction to another.

Figure 7. The argon He-α line seen along the y-axis shows little difference between the case with (dashed) and without (solid) the opacity due to carbon in the plastic shell.

Figure 8. The upper state populations for all three lines are shown as a function of position along the y-axis. The argon Ly-α line has a broad peak, the argon He-α line has a narrow peak near the outer edge of the fuel, and the titanium He-α line has a peak that is one zone wide and can't be distinguished in this plot.

Figure 9. The upper state density (normalized to its maximum) for the titanium He-α line is shown as a function of position along several radial directions. The

strength and location of the titanium emission is very sensitive to the direction. The density along the y-axis is 7% of the peak and it is even smaller in the other directions. This strong variability corresponds to the patchy nature of the titanium emission in figure 6.

Figure 10. The spectrum at the time of peak emission for all three capsules (viewed along the +x-axis). The 50 atmosphere Omega capsule has stronger He-α satellite emission than the Nova capsule, while the He-α line has the same strength.

Figure 11. The spectrum from the Nova capsule in four directions shows large variations. The spectrum from the Omega capsule (not shown) is essentially the same in all directions.

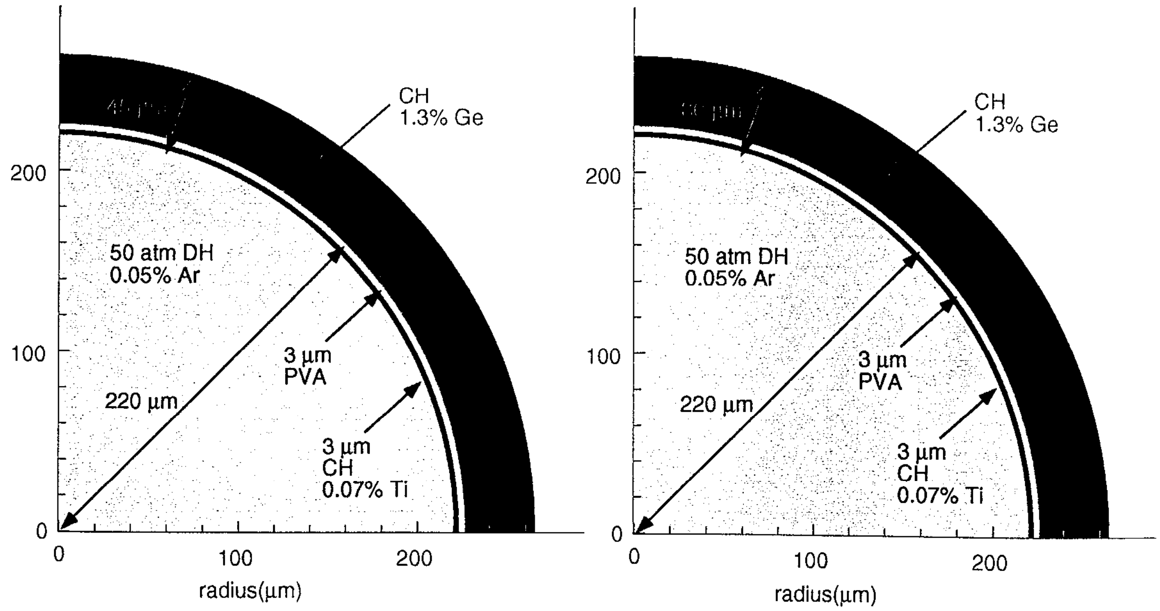
CH
1.3% Ge
50 atm DH
0.05% Ar
3 μm
PVA
220 μm
3 μm
CH
0.07% Ti
0
100
200
radius(μm)
CH
1.3% Ge
50 atm DH
0.05% Ar
3 μm
PVA
220 μm
3 μm
CH
0.07% Ti
0
100
200
radius(μm)

Figure 1

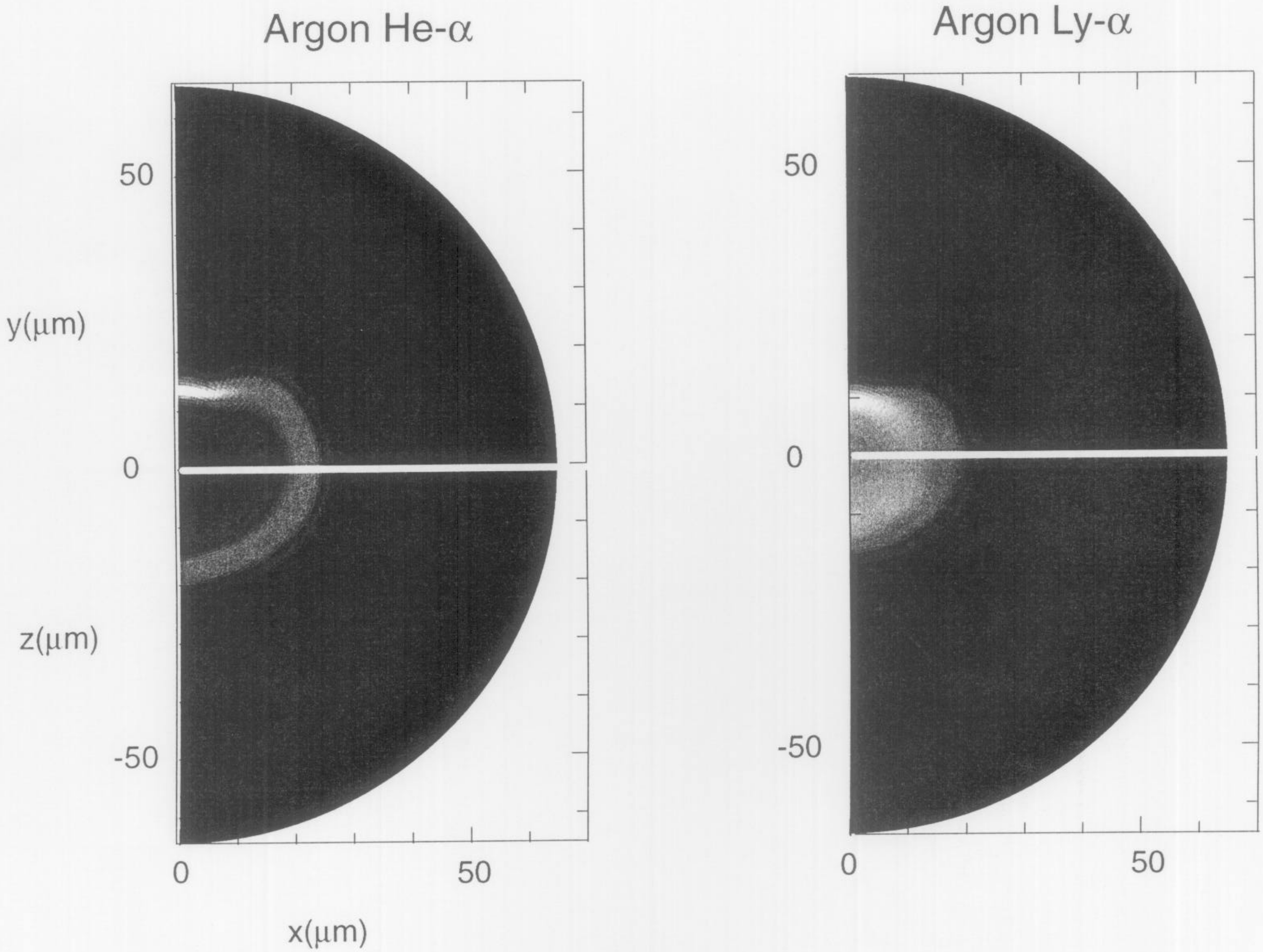

Figure 2

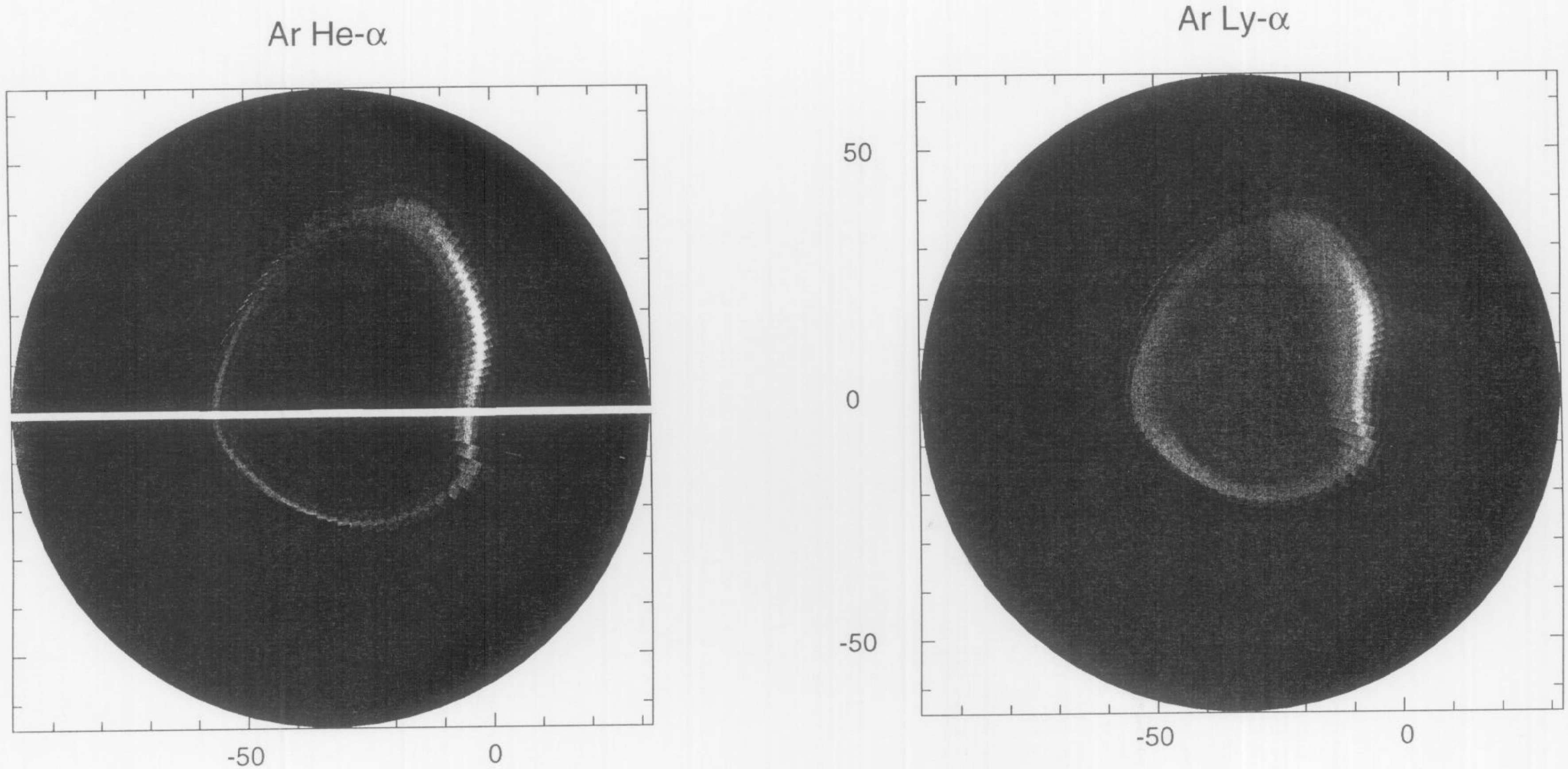

Figure 3

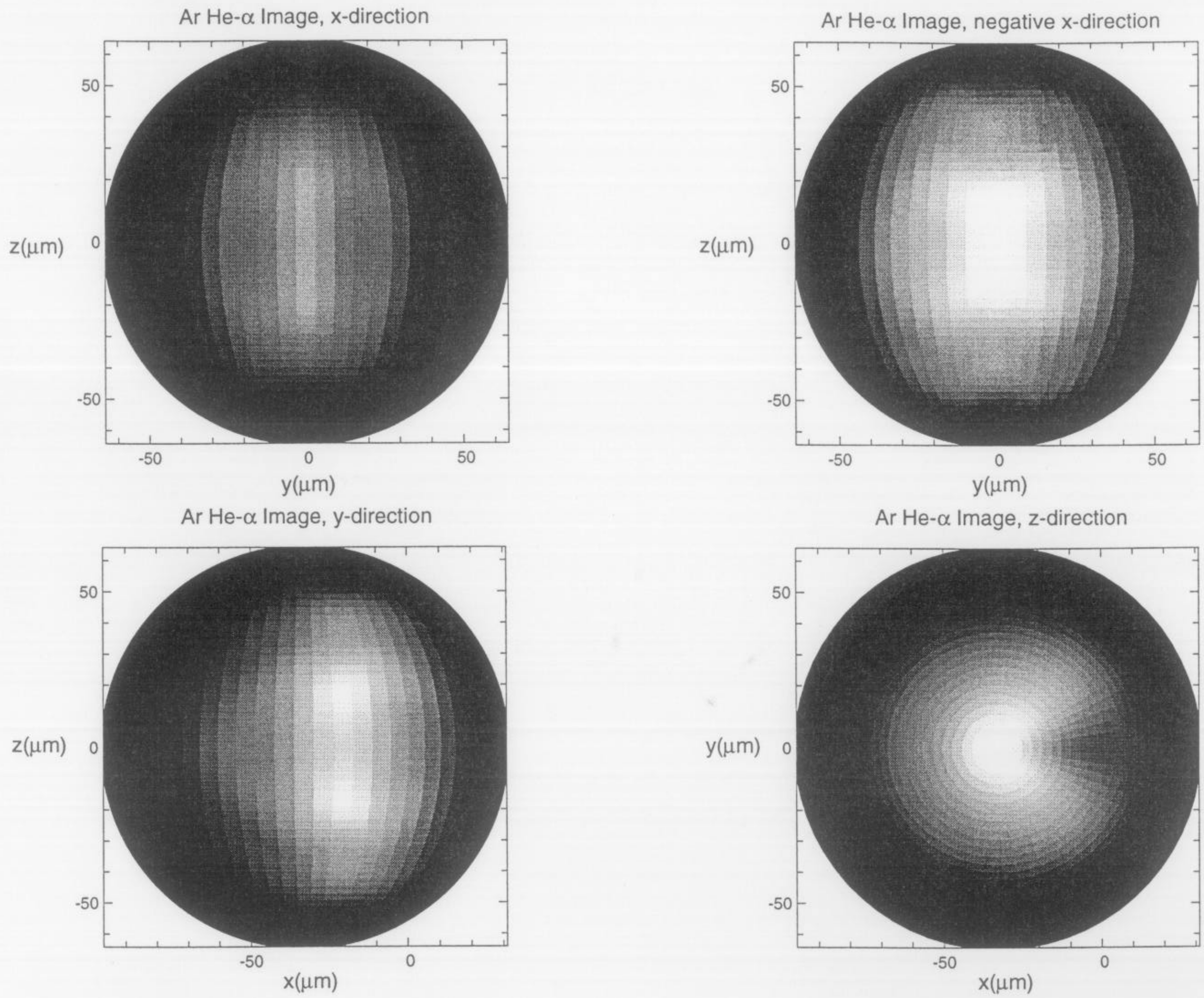
Ar He-α Image, x-direction
z(μm)
y(μm)
Ar He-α Image, negative x-direction
z(μm)
y(μm)
Ar He-α Image, y-direction
z(μm)
x(μm)
Ar He-α Image, z-direction
y(μm)
x(μm)
50
0
-50

Figure 4

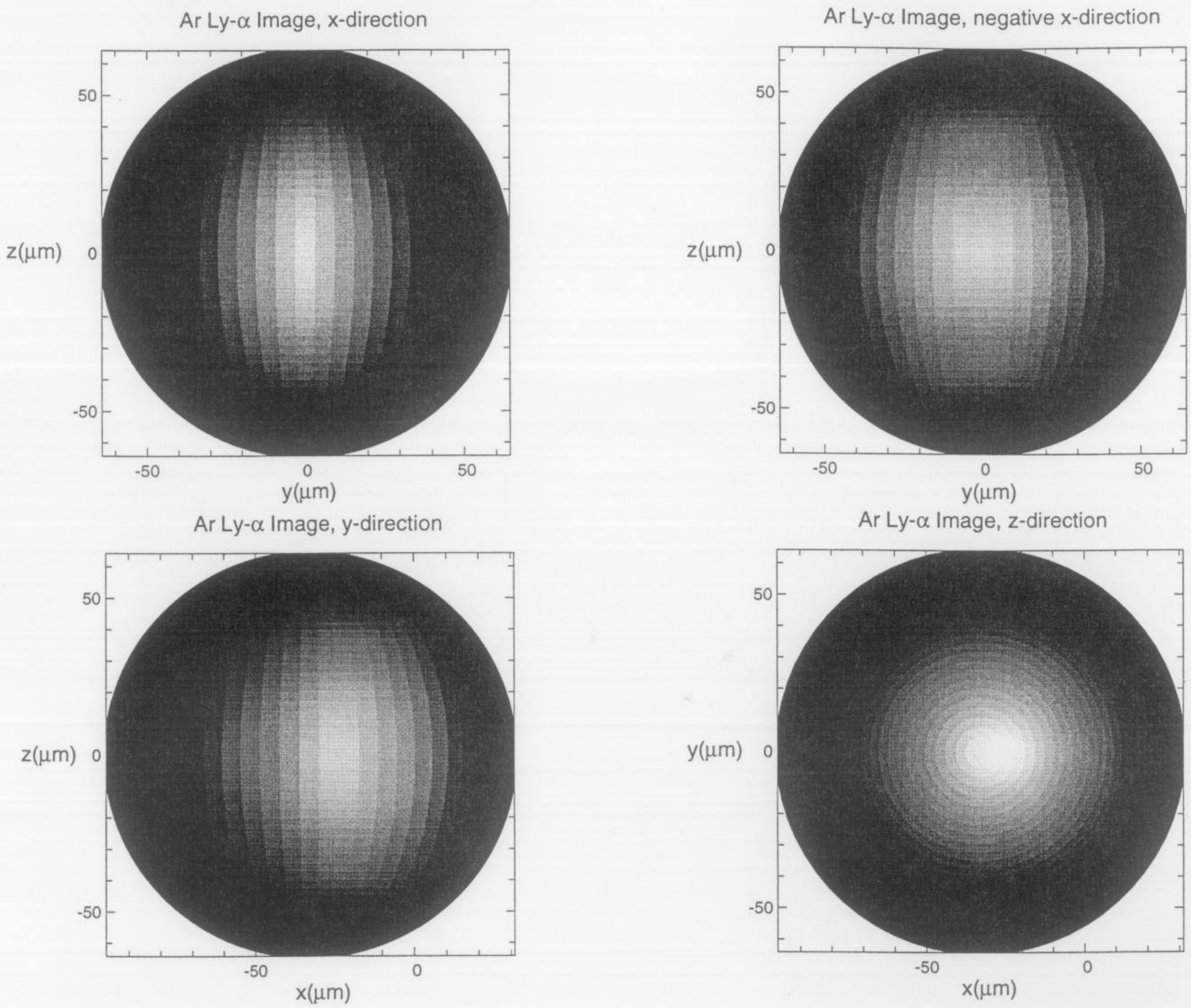
Ar Ly-α Image, x-direction
Ar Ly-α Image, negative x-direction
Ar Ly-α Image, y-direction
Ar Ly-α Image, z-direction
z(μm)
y(μm)
x(μm)
50
0
-50

Figure 5

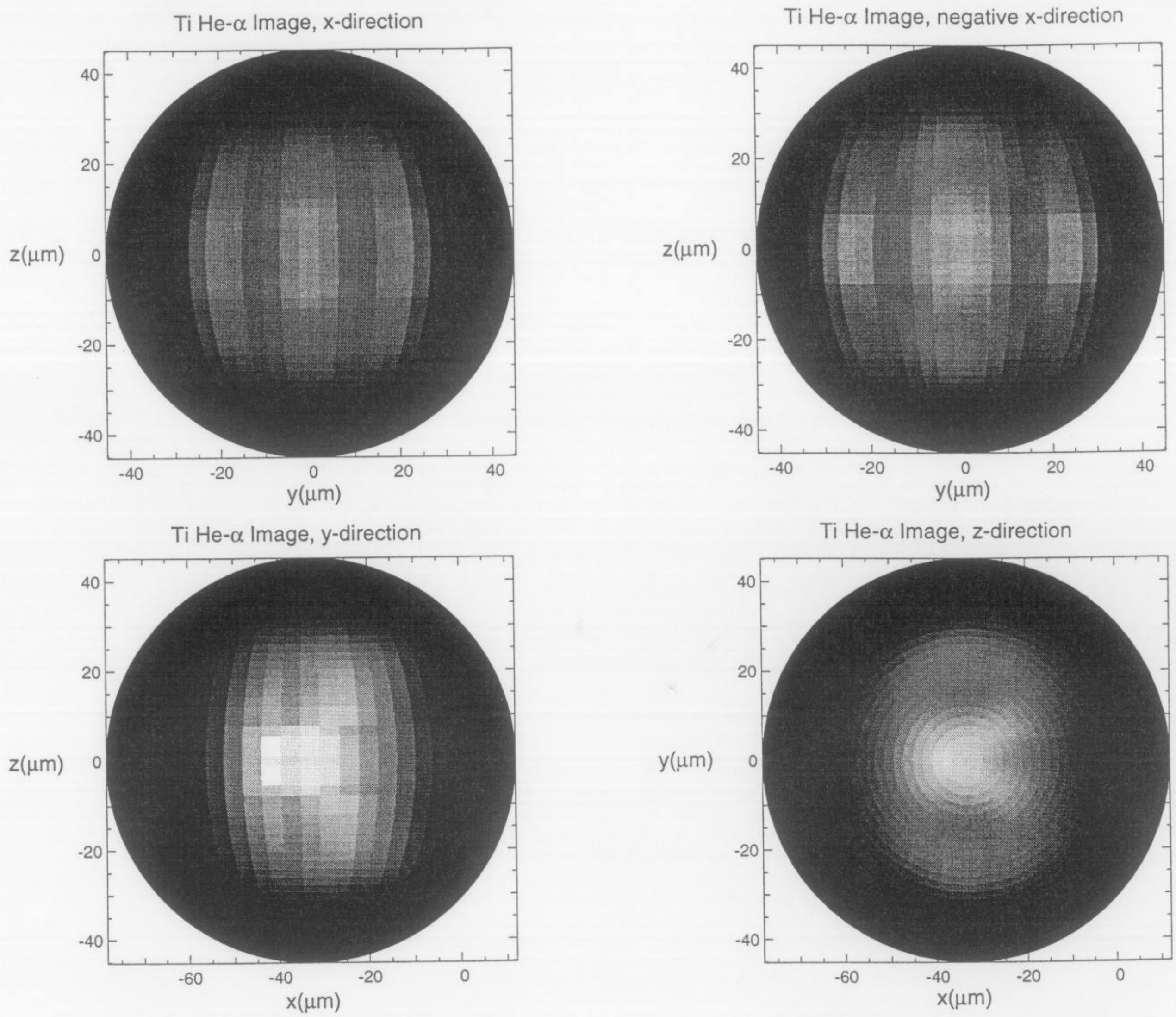

Ti He-α Image, x-direction
z(μm)
y(μm)
40
20
0
-20
-40
Ti He-α Image, negative x-direction
z(μm)
y(μm)
Ti He-α Image, y-direction
z(μm)
x(μm)
-60
-40
-20
0
Ti He-α Image, z-direction
y(μm)
x(μm)

Figure 6

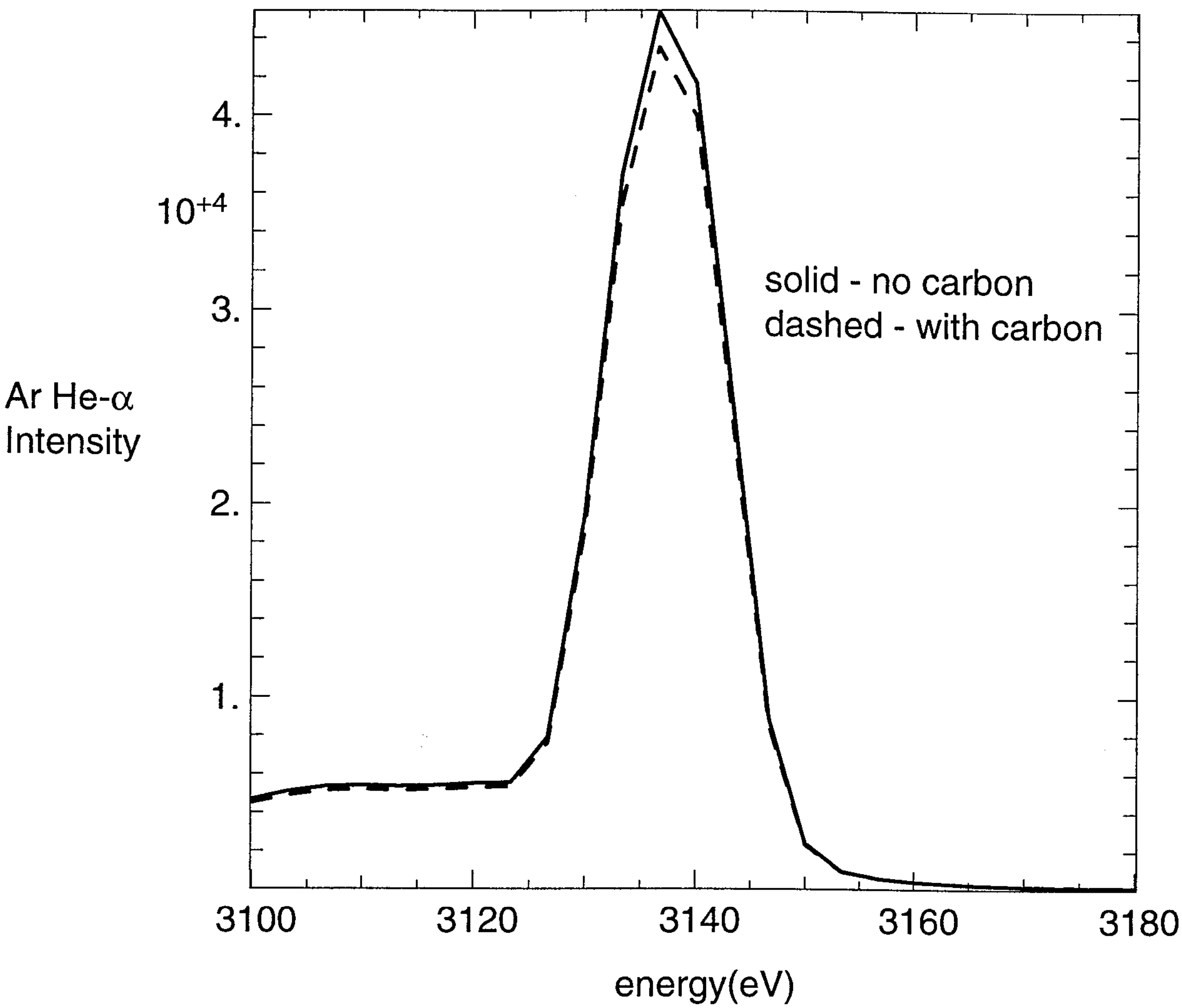

4.
10+4
3.
2.
1.
Ar He-α
Intensity
solid - no carbon
dashed - with carbon
3100
3120
3140
3160
3180
energy(eV)

Figure 7

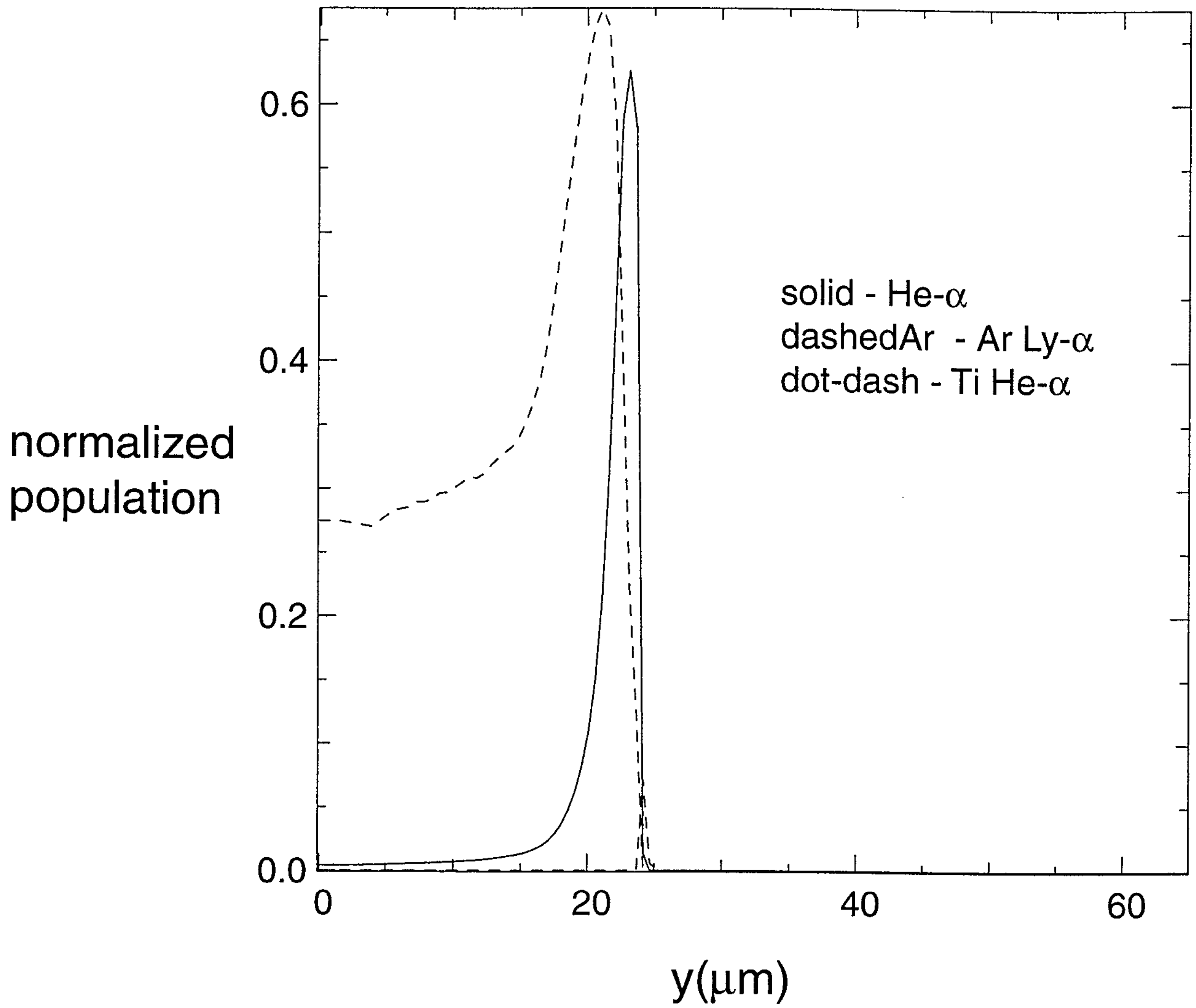

normalized
population
0.0
0.2
0.4
0.6
0
20
40
60
y(μm)
solid - He-α
dashedAr - Ar Ly-α
dot-dash - Ti He-α

Figure 8

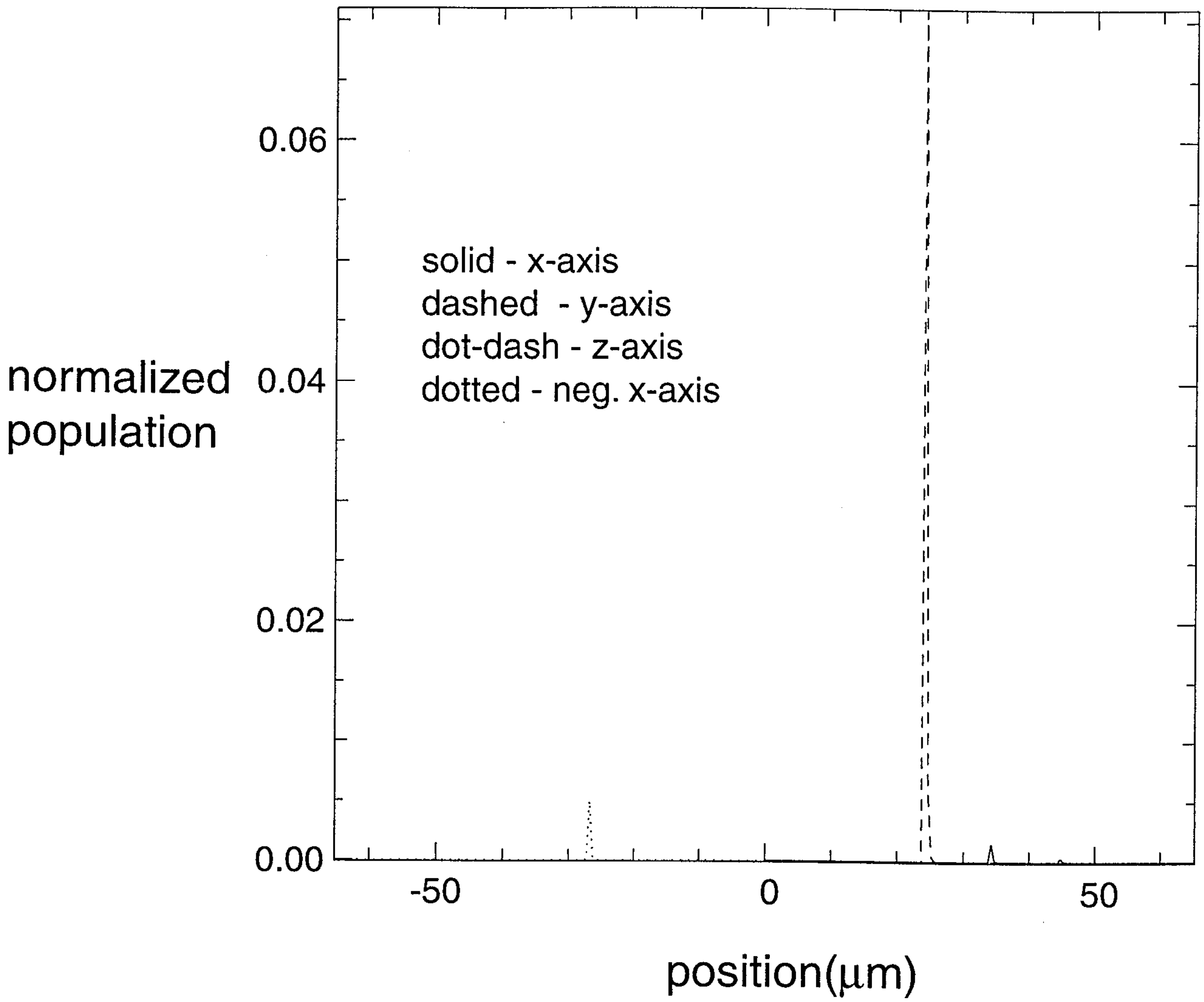

normalized population
0.06
0.04
0.02
0.00
solid - x-axis
dashed - y-axis
dot-dash - z-axis
dotted - neg. x-axis
-50
0
50
position(μm)

Figure 9

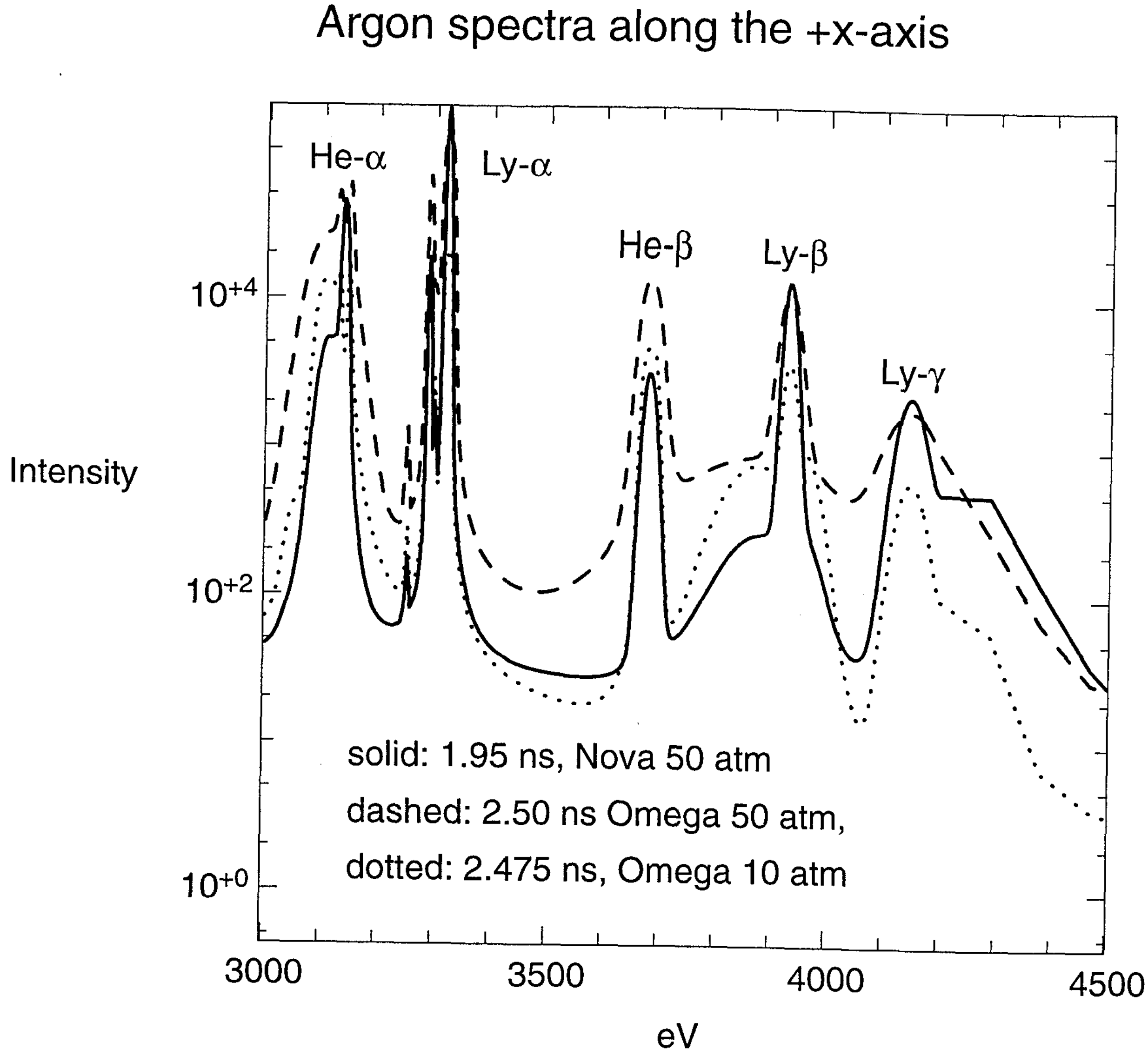
Argon spectra along the +x-axis
He-α
Ly-α
He-β
Ly-β
Ly-γ
10+4
10+2
10+0
Intensity
solid: 1.95 ns, Nova 50 atm
dashed: 2.50 ns Omega 50 atm,
dotted: 2.475 ns, Omega 10 atm
3000
3500
4000
4500
eV

Figure 10

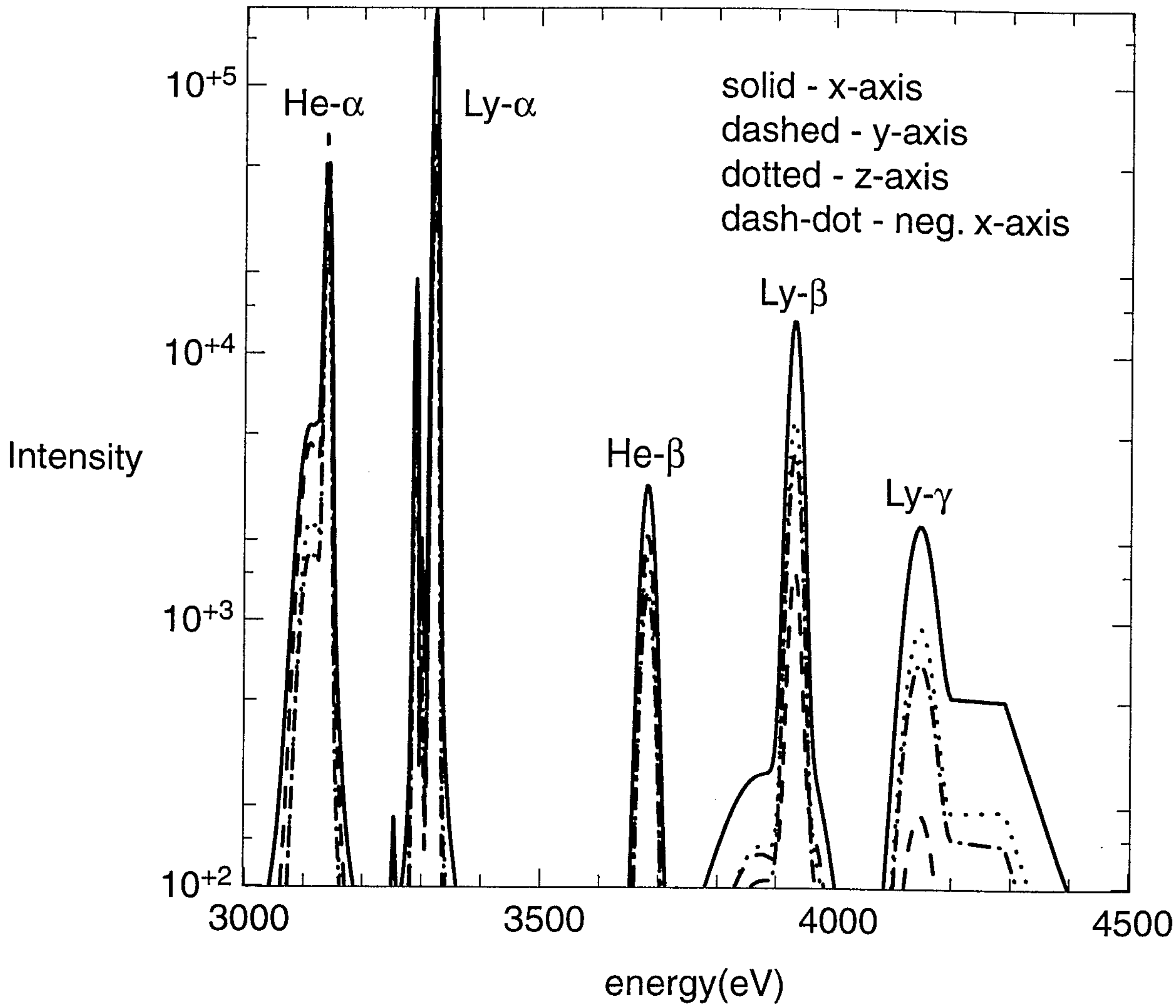

He-α
Ly-α
solid - x-axis
dashed - y-axis
dotted - z-axis
dash-dot - neg. x-axis
Ly-β
He-β
Ly-γ
Intensity
10+5
10+4
10+3
10+2
3000
3500
4000
4500
energy(eV)

Figure 11